

Deconvolutional Method Utilizing Power Variable Point Spread Function for Resolution Degradation Mitigation in SBS-Based Optical Spectrum Analyzer

Zi Liang , Yuming Zhang , Haoyu Wang , Changjian Ke , and Deming Liu 

Abstract—High-resolution optical spectroscopy is a significant approach to reveal the inherent laws of devices and systems. Although optical spectrum analyzer (OSA) based on stimulated Brillouin scattering (SBS) has achieved a resolution of ~ 10 pm, when the signal power increases, the Brillouin gain spectrum (BGS) will saturate and cause resolution degradation. In order to solve this problem, we introduce shape factor k to describe the variation of BGS with signal power, and adopt the BGS as the point spread function (PSF). Then the signal is divided into several intervals with equal frequency spacing, where the BGS does not change. On this basis, we perform the Jansson-Van Cittert (JVC) algorithm to complete deconvolution in each interval with power variable PSF. The proposed method is used to test the periodic signal in SBS-OSA. Experimental results show that the proposed method can improve the spectral resolution from 22 MHz to 11 MHz when the frequency interval is 14 MHz and the signal power is -5 dBm.

Index Terms—Deconvolution, power variable PSF, resolution degradation, SBS-based OSA, gain saturation.

I. INTRODUCTION

HIGH-RESOLUTION optical spectroscopy can obtain more details of signal spectrum, thus revealing more inherent changes of devices and systems. Therefore, it has a wide range of applications in signal characterization of optical communication systems [1], [2], [3], high accuracy optical sensing [4], laser sources characterization [5], [6], optical frequency combs and other device performance evaluation [7], [8], [9], etc. The traditional OSA resolution based on diffraction grating is ~ 20 pm [10], which cannot meet above requirements. SBS-based OSA (SBS-OSA) has attracted increasing attention owing to its ability to achieve high-resolution spectral analysis.

The most important part of the SBS-OSA is SBS-based narrow-band optical filter (SBS-NBOF), and the frequency response can best reflect its characteristics. The frequency response characteristics of the SBS effect are affected by factors,

Manuscript received 14 September 2023; revised 22 November 2023; accepted 14 December 2023. Date of publication 19 December 2023; date of current version 29 December 2023. This work was supported by the National Natural Science Foundation of China under Grant 61975063. (Corresponding author: Changjian Ke.)

Zi Liang, Yuming Zhang, and Haoyu Wang are with the School of Optical and Electronic Information, Huazhong University of Science and Technology, Wuhan 430074, China (e-mail: zilianghust@hust.edu.cn; m202172916@hust.edu.cn; wanghaoyu@hust.edu.cn).

Changjian Ke and Deming Liu are with the School of Optical and Electronic Information, Huazhong University of Science and Technology, Wuhan 430074, China, and also with Wuhan National Laboratory for Optoelectronics, Wuhan 430074, China (e-mail: cjke@mail.hust.edu.cn; dmliu@mail.hust.edu.cn).

Digital Object Identifier 10.1109/JPHOT.2023.3344193

e.g., pump power, polarization state between signal and pump light, and sweep speed. In order to solve the frequency response distortion caused by the mismatch between polarization state of the signal light and the pump light, a polarization-and wavelength-independent SBS-NBOF structure has been proposed, which can alleviate the influence of output signal fluctuation caused by the polarization state change [11]. Aiming at the problem of frequency response distortion caused by too fast pump tuning speed, a spectral distortion compensation method based on R-L deconvolution algorithm has been proposed to improve the feasible sweep speed [12]. In consideration of the dynamic range degradation of SBS-NBOF due to gain saturation, a hardware structure based on pump splitting dual-stage configuration has been proposed to improve the selectivity of frequency response [13], [14]. Due to the gain saturation phenomenon, BGS will be affected by the signal power, so that the output signal optical spectrum of the SBS-OSA will be broadened, which will eventually lead to spectral resolution degradation. However, the primary solution to this problem now is to optimize the hardware structure of SBS-NBOF.

In this paper, we propose a deconvolutional method utilizing power variable PSF to mitigate the resolution degradation in SBS-OSA. Firstly, it is assumed that the input signal is a set of discrete spectral lines with equal frequency spacing and unequal power. Then the shape factor k is introduced to describe the variation of BGS with respect to signal power, hereby the expression of the output signal is given. On this basis, the signal is divided into several intervals. On each interval the signal power doesn't change, thus the corresponding shape factor k and PSF doesn't change either. Therefore, on each interval the JVC algorithm can be performed. Then the experimental set-up is constructed, the relationship between shape factor k and signal power is calibrated by using the single-frequency input signal. Finally, the effectiveness of the proposed method is validated for the periodic signal. Experimental results show that for periodic signals with a frequency interval of 14MHz and a power of -5 dBm, the resolution is improved from 22 MHz to 11 MHz by proposed method.

II. PRINCIPLES

In the SBS-OSA, a moving grating is formed by the electrostriction effect after the pump light is incident into the fiber. At this time, when the signal light input into the fiber in the opposite

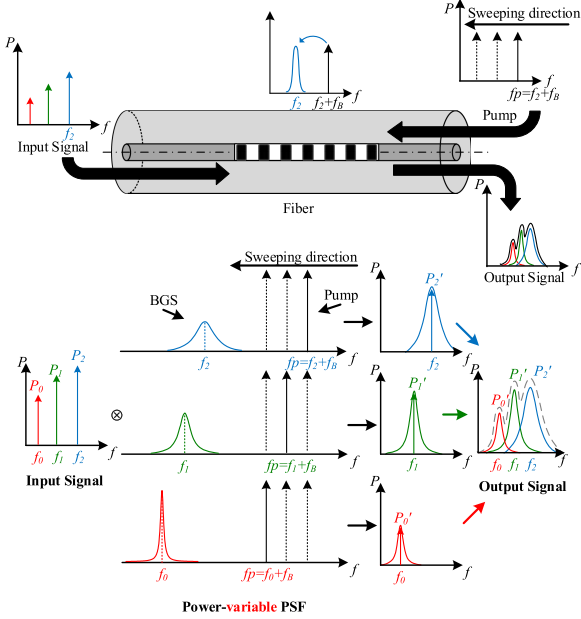


Fig. 1. Schematic diagram of the influence of the PSF on the output signal with the change of power.

direction of the pump light, the signal within the BGS bandwidth will be amplified by the SBS effect, while the remaining signals that are not within the gain bandwidth will be attenuated by the link loss. Therefore, this process forms an equivalent NBOF. On this basis, by continuously tuning the frequency of the pump light, different frequency components in the signal can be filtered out. By covering the frequency range of the input signal, the spectral analysis can be completed.

Since the BGS largely determines the characteristics of the output signal, if the BGS varies with input power, the output signal will also be affected, as shown in Fig. 1. Assuming that the input signal is a set of discrete spectral lines with the same frequency spacing and different power, with the tuning of the pump frequency, different BGS will be excited at the corresponding frequency. Since SBS-OSA usually works in a constant pump power state and the fiber length is fixed, the excited BGS is mainly related to the signal power. The corresponding frequency components of the input signal are amplified and filtered after the equivalent filtering of the BGS. The amplification depends on the signal power and BGS at this frequency. Due to the different signal power at different frequencies, the corresponding BGS also change. For higher power signals, the effect of gain saturation reduces the gain of the BGS and increases its bandwidth, resulting in an increase in the valley-to-peak ratio of the output signal, which eventually leads to the spectral resolution degradation.

For the convenience of analysis, it is assumed that the input signal is a set of discrete spectral lines with the same frequency interval and different powers [15]:

$$P_{in}(f) = \sum_i P_s(f_i) \delta(f - f_i) \quad (1)$$

where the $f_i = i\Delta f$, Δf is the interval between the spectral lines, $P_s(f_i)$ is the power at the corresponding spectral line, $\delta(f)$ is the pulse function.

The input signal is amplified by the SBS effect with the pump light in the fiber, and the process of sweeping the frequency and reconstructing the spectrum can be regarded as the convolution of the BGS $H(f)$ and the input signal $P_{in}(f)$.

$$P_{out}(f) = P_{in}(f) * H(f) \quad (2)$$

For the SBS-OSA, the system transfer function is mainly determined by the BGS in the fiber, which usually has a Lorentzian profile [16]. However, in fact, the shape of BGS changes with pump power, signal power and fiber length, especially the signal power in SBS-OSA. In order to describe the shape of BGS changing with signal power, we introduce a shape factor k related to the signal power, which can be abbreviated as $k = k(P_s(f_i))$. Then the BGS can be expressed as [16]:

$$H(f, k) = g_0 \left[\frac{(\Delta f_B / 2\sqrt{2^{1/k} - 1})^2}{(f - f_B)^2 + (\Delta f_B / 2\sqrt{2^{1/k} - 1})^2} \right]^k \quad (3)$$

where g_0 is peak Brillouin gain, f_B is Brillouin shift, Δf_B is FWHM of BGS.

For the spectral lines at different frequencies of the signal, assuming that the frequency interval is small, the change of the signal power in this interval range can be ignored, hence the corresponding BGS shape does not change. According to the spectral reconstruction process, the output signal spectrum can be expressed as:

$$P_{out}(f) = \sum_i P_s(f_i) H(f - f_i, k) \quad (4)$$

$$H(f - f_i, k) = g_0 \left[\frac{(\Delta f_B / 2\sqrt{2^{1/k} - 1})^2}{[f - (f_B + f_i)]^2 + (\Delta f_B / 2\sqrt{2^{1/k} - 1})^2} \right]^k \quad (5)$$

When input signal is single frequency at f_1 , (5) can be rewritten as:

$$H(f - f_1, k) = g_0 \left[\frac{(\Delta f_B / 2\sqrt{2^{1/k} - 1})^2}{[f - (f_B + f_1)]^2 + (\Delta f_B / 2\sqrt{2^{1/k} - 1})^2} \right]^k \quad (6)$$

where $k = k(P_s(f_1))$.

Correspondingly, the output signal can be expressed as:

$$P_{out}(f) = P_s(f_1) H(f - f_1, k) \approx H(f - f_1, k) \quad (7)$$

Therefore, the system transfer function, i.e., the BGS, can be obtained by analyzing the output signal when a single-frequency signal is input.

The input and output of the SBS-OSA satisfy the convolution relation, and BGS corresponds to PSF. In order to mitigate the resolution degradation caused by the correlation between the PSF and the input signal power, and to recover the input signal without distortion, the deconvolutional method is a valid way.

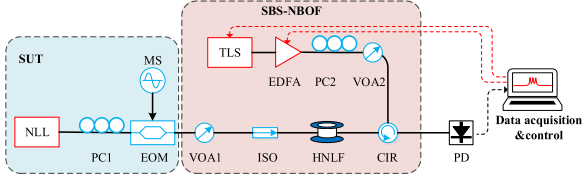


Fig. 2. Diagram of the PSF and SUT measurement device. NLL: narrow linewidth laser; PC: polarization controller; EOM: electro-optic modulator; MS: microwave source; VOA: variable optical attenuator; ISO: optical isolator; TLS: tunable laser source; CIR: circulator; HNLF: highly nonlinear fiber.

We adopt the JVC algorithm, which is a commonly used and effective algorithm in the spectrometer signal deconvolutional method [17], [18].

In [17], the iterative formula of the JVC algorithm can be expressed as follows:

$$\hat{P}_{in}^{(m+1)}(f) = \hat{P}_{in}^{(m)}(f) + r \left(\hat{P}_{in}^{(m)}(f) \right) \left(P_{out}(f) - \sum_i H(f - f_i, k) \hat{P}_s^{(m)}(f_i) \right) \quad (8)$$

where $\hat{P}_{in}^{(m)}(f)$ is the input signal at the m -th iteration, $r(\hat{P}_{in}^{(m)}(f))$ is the slack function, used to limit noise to implement constraints on solutions, m is the current times of iterations. Usually we set $\hat{P}_{in}^{(0)}(f) = P_{out}(f)$.

In the JVC algorithm, the PSF will not change with power in the iterative process, i.e., $H(f - f_i, k) = H(f - f_1, k)$, $k = k(\hat{P}_s^{(m)}(f_1))$. Under the circumstance that the PSF will change with power, the traditional JVC algorithm is not applicable for SBS-OSA. Therefore, a deconvolutional method utilizing power variable PSF is proposed. First, the input signal is divided into several intervals with equal frequency interval. In each interval, the change of signal power can be ignored, so the corresponding BGS does not change, i.e., there is a shape factor k corresponding to the signal power uniquely. Therefore, the JVC algorithm can be applied to deconvolution in each interval. The biggest difference with the JVC algorithm is that the PSF in (6) will change with signal power. The iterative formula of the proposed method as follows:

$$\hat{P}_{in}^{(m+1)}(f) = \hat{P}_{in}^{(m)}(f) + r \left(\hat{P}_{in}^{(m)}(f) \right) \left(P_{out}(f) - \sum_i H_{pv}(f - f_i, k) \hat{P}_s^{(m)}(f_i) \right) \quad (9)$$

where, $H_{pv}(f - f_i, k)$ is given in (5), $k = k(\hat{P}_s^{(m)}(f_i))$.

III. EXPERIMENTAL SETUP AND RESULTS

According to (7), when the input signal is single frequency, it can be equivalent to a pulse function, so the output signal can be approximately characterized by the system transfer function, i.e., the BGS. Therefore, we obtain the PSF by a single-frequency input signal under different input signal powers. The experimental setup is shown in Fig. 2.

In the experiment, the narrow linewidth laser (SANTEC TSL-710) used to generate the signals to be measured has a linewidth of ~ 100 kHz, and the central wavelength is 1550 nm.

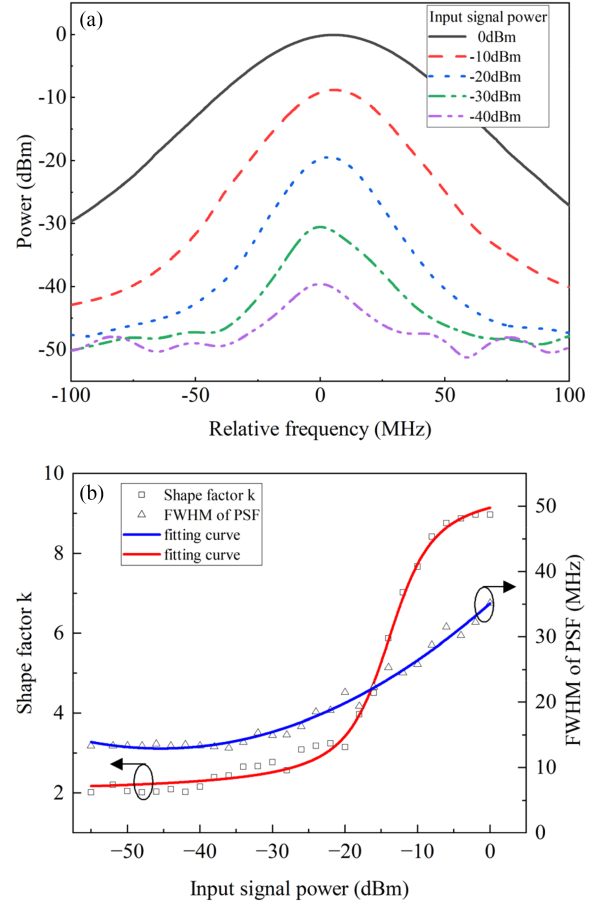


Fig. 3. Variation of PSF with input power: (a) output spectrum; (b) bandwidth and shape factor k .

EOM and MS are used to modulate and generate various signals to be measured, and the signal power is controlled by the variable optical attenuator VOA1. The core component of SBS-OSA is SBS-NBOF, as shown in the red region in Fig. 2. The tunable laser (LUNA Phoenix 1200) used for pumping has a linewidth of ~ 100 kHz and the wavelength sweeping range is 1549.5 nm–1550.5 nm. EDFA is used to amplify the pump light, usually working in constant power mode. PC2 is used to adjust the polarization state of the pump light to obtain the maximum gain, and then the pump power is adjusted by VOA2. Highly nonlinear fiber (HNLF) is specially designed for SBS narrow-band filtering. It is characterized by a single-peak BGS with a peak Brillouin gain coefficient of $2.45 \text{ m}^{-1} \cdot \text{W}^{-1}$, and a BGS bandwidth of ~ 10 MHz. The output signal is received by the PD through the circulator, and then collected by the NI PXIe-5122 to obtain the spectrum.

Firstly, we generate a signal with a linewidth of ~ 100 kHz through NLL. Since its linewidth is much smaller than the BGS bandwidth, it can be approximated as a single-frequency input signal. The output spectrum under different power is obtained by changing the input signal power. As shown in Fig. 3(a), when the input power increases, the bandwidth of the BGS gradually increases, which is also an important reason for the spectral resolution degradation.

Then we fit the power variable PSF model based on the experimentally measured PSF to obtain the corresponding fitting parameters. For the signal with input power P_1 , the corresponding PSF H_1 can be obtained, and H_1 corresponds to shape factor k_1 and bandwidth according to (6). The PSF under different input signal powers can be obtained by changing the input power. The relationship between the shape factor k and PSF bandwidth with the input signal power is shown in Fig. 3(b), and the bandwidth change of the PSF is basically consistent with known reports [12]. After obtaining the shape factor k and bandwidth under partial input signal power, the shape factor k and bandwidth curves that change continuously can be obtained by fitting the curves. Then the power variable PSF can be obtained and used in the proposed deconvolutional method.

The resolution of the spectrometer is usually judged by the Rayleigh criterion [19], i.e., when the valley-to-peak ratio is less than 0.8, the two close spectral lines can be distinguished. The lower the valley-to-peak ratio, the better the spectral resolution. Based on the Rayleigh criterion, we design an experiment to verify the effect of the proposed deconvolutional method. We select the signal with a certain periodic structure of the spectrum as the input signal and generate it through the experimental setup mentioned above. The MS can generate input signals with different frequency intervals, which are selected from 11 to 26 MHz to calculate the resolution according to the Rayleigh criterion. Since the spectral width of the periodic signal is larger than that of the single-frequency signal, in order to make the corresponding peak power of the periodic signal consistent with the single-frequency signal, the total power of integration of the periodic signal is therefore in the range of -35 dBm \sim -5 dBm. Fig. 4(a) shows the spectrum of one set of input signals at different input powers with a frequency interval of 14 MHz. As a contrast, Fig. 4(b) shows the corresponding spectrum processed by the proposed deconvolutional method. It indicates that the valley-to-peak ratio of the signal spectrum is significantly reduced with the proposed method at each input signal power, i.e., the spectral resolution degradation caused by gain saturation is effectively mitigated.

Fig. 5 shows the valley-to-peak ratio with and without the proposed method for periodic signals under different frequency intervals and different input signal powers. According to the Rayleigh criterion, the resolution under the corresponding signal power can be obtained by the intersection of the valley-to-peak ratio with frequency interval curve and the straight line with a valley-to-peak ratio of 0.8. The figure illustrates that without the proposed method, as the input signal power increases, the valley-to-peak ratio at each power gradually increases, resulting in a gradual deterioration of the resolution. On the other hand, after using the proposed method, the peak-to-valley ratio curve of each power is significantly smaller than that without the proposed method. Additionally, the intersection point is concentrated at a smaller frequency, thus the resolution value is significantly reduced. From the above we can know that the resolution degradation has been effectively mitigated.

Furthermore, the effect of the proposed method on the resolution degradation mitigation with other resolution degradation mitigation method is compared. The hardware method is based

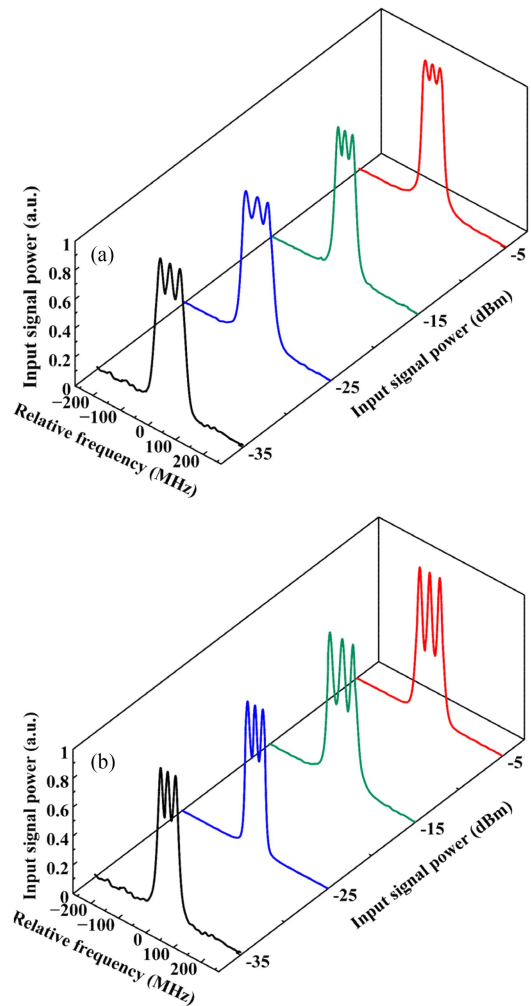


Fig. 4. Under different input powers, the normalized periodic signal spectrum with a frequency interval of 14 MHz: (a) without proposed method; (b) with proposed method.

on the splitting pump dual-stage structure proposed in [13]. According to the device structure in [13], we additionally build an SBS-OSA with dual-stage pump structure, whose system parameters are selected when the dual-stage SBS-OSA is working at the overall best performance. The resolution measurement method of dual-stage SBS-OSA is consistent with that in this paper. Fig. 6 shows the variation of SBS-OSA resolution with the input signal power when different methods are used. Firstly, for the proposed method, the resolution is significantly reduced compared with the resolution that unprocessed, and it changes little with the signal power, indicating that the proposed method has a good effect on the resolution degradation mitigation. Because the higher power signal will suffer more serious gain saturation, while the effect of the proposed method is related to the input signal power, eventually leading to the downtrend of the red line. Then, for the hardware method, the resolution under each signal power is reduced to a certain extent by optimizing the hardware structure, but the resolution is reduced less as the signal power changes greatly. The results show that in SBS-OSA, the proposed method is better in mitigating the resolution

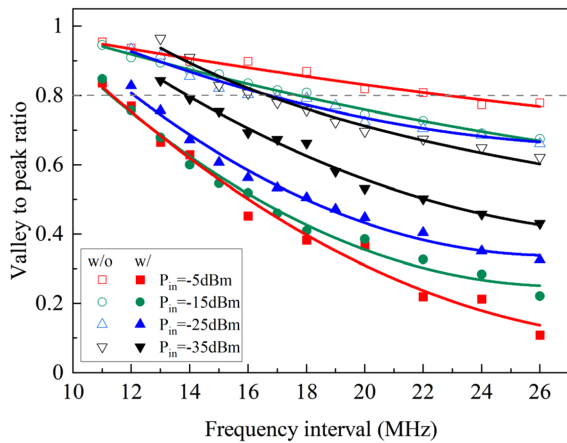


Fig. 5. Relationship between the valley-to-peak ratio of the normalized periodic signal and the frequency interval under different powers.

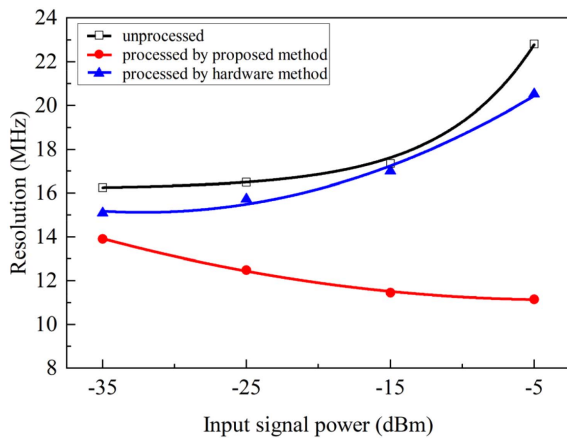


Fig. 6. Relationship between the resolution of the SBS-OSA and the input signal power with different resolution degradation mitigation methods.

degradation than the hardware method. From the perspective of comprehensive effect and system complexity, the proposed method is an optimal solution.

IV. CONCLUSION

In summary, we propose a deconvolutional method utilizing power variable PSF, which can effectively mitigate the spectral resolution degradation caused by SBS gain saturation in SBS-OSA. The shape factor k is introduced to describe the variation of BGS, under the circumstances that the input signal is a set of discrete spectral lines with equal frequency spacing and unequal power at the frequency, the expression of the output signal is given. Then a deconvolutional method utilizing power variable PSF is proposed. Firstly, the signal is divided into several intervals, in which the signal power doesn't change, thus the corresponding shape factor k and PSF doesn't change either. After that, the JVC algorithm is performed in each interval to iterate. Next, the experimental set-up is constructed and the relationship between shape factor k and signal power is experimentally calibrated by using the single-frequency input

signal. To validate the effectiveness of the proposed algorithm, quantitative evaluation illustrates that for periodic signals with a frequency interval of 14 MHz and a power of -5 dBm, the resolution of SBS-OSA is improved from 22 MHz to 11 MHz. The proposed method can make SBS-OSA suitable for larger input power range, so that it can be more stably and accurately applied to the signal characterization of optical communication systems and the performance evaluation of laser light sources, optical frequency combs and other devices.

REFERENCES

- [1] B. Shariati, M. Ruiz, J. Comellas, and L. Velasco, "Learning from the optical spectrum: Failure detection and identification," *J. Lightw. Technol.*, vol. 37, no. 2, pp. 433–440, Jan. 2019.
- [2] A. P. Vela et al., "Soft failure localization during commissioning testing and lightpath operation," *J. Opt. Commun. Netw.*, vol. 10, no. 1, pp. A27–A36, Jan. 2018.
- [3] F. Locatelli, K. Christodoulopoulos, M. S. Moreolo, J. M. Fàbrega, and S. Spadaro, "Machine learning-based in-band OSNR estimation from optical spectra," *IEEE Photon. Technol. Lett.*, vol. 31, no. 24, pp. 1929–1932, Dec. 2019.
- [4] B. Yang, H. Chi, S. Yang, Z. Cao, J. Ou, and Y. Zhai, "Broadband microwave spectrum sensing based on photonic RF channelization and compressive sampling," *IEEE Photon. J.*, vol. 12, no. 1, Feb. 2020, Art. no. 5500109.
- [5] Z. Yuan, H. Wang, L. Wu, M. Gao, and K. Vahala, "Linewidth enhancement factor in a microcavity Brillouin laser," *Optica*, vol. 7, no. 9, pp. 1150–1153, Sep. 2020.
- [6] K. Liu et al., "Fundamental linewidth of an AlN microcavity Raman laser," *Opt. Lett.*, vol. 47, no. 17, pp. 4295–4298, Sep. 2022.
- [7] A. Atieh, B. Kanwal, S. Ghafoor, M. Sajid, and J. Mirza, "Design and analysis of redundant optical comb for data center networks," *Opt. Quantum Electron.*, vol. 55, no. 1, Dec. 2023, Art. no. 58.
- [8] T. Fortier and E. Baumann, "20 years of developments in optical frequency comb technology and applications," *Commun. Phys.*, vol. 2, no. 1, Dec. 2019, Art. no. 153.
- [9] B. Redding, J. D. McKinney, R. T. Schermer, and J. B. Murray, "High-resolution wide-band optical frequency comb control using stimulated Brillouin scattering," *Opt. Exp.*, vol. 30, no. 12, pp. 22097–22106, Jun. 2022.
- [10] Y. Dong et al., "Sub-MHz ultrahigh-resolution optical spectrometry based on Brillouin dynamic gratings," *Opt. Lett.*, vol. 39, no. 10, pp. 2967–2970, May 2014.
- [11] C. Xing et al., "Polarization- and wavelength-independent SBS-based filters for high resolution optical spectrum measurement," *Opt. Exp.*, vol. 25, no. 18, pp. 20969–20982, Sep. 2017.
- [12] Y. Zhong et al., "Frequency response of a continuously tuning narrow-band optical filter based on stimulated Brillouin scattering," *Opt. Exp.*, vol. 29, no. 19, pp. 30307–30318, Sep. 2021.
- [13] K. Zhang et al., "High-input dynamic range and selectivity stimulated Brillouin scattering-based microwave photonic filter utilizing a dual-stage scheme," *Opt. Lett.*, vol. 42, no. 17, pp. 3287–3290, Sep. 2017.
- [14] L. Yi et al., "Polarization-independent rectangular microwave photonic filter based on stimulated Brillouin scattering," *J. Lightw. Technol.*, vol. 34, no. 2, pp. 669–675, Jan. 2016.
- [15] J. Debeau, B. Kowalski, and R. Boittin, "Simple method for the complete characterization of an optical pulse," *Opt. Lett.*, vol. 23, no. 22, pp. 1784–1786, Nov. 1998.
- [16] A. Villafranca, J. Lázaro, Í. Salinas, and I. Garcés, "Stimulated Brillouin scattering gain profile characterization by interaction between two narrow-linewidth optical sources," *Opt. Exp.*, vol. 13, no. 19, pp. 7336–7341, Sep. 2005.
- [17] P. A. Jansson, *Deconvolution of Images and Spectra*. Chelmsford, MA, USA: Courier Corporation, 2014.
- [18] B. William, *Deconvolution of Absorption Spectra*. Amsterdam, The Netherlands: Elsevier, 2012.
- [19] P. R. Griffiths, *Handbook of Vibrational Spectroscopy*. Hoboken, NJ, USA: Wiley, 2002.